Research Article

SOHAG JOURNAL OF SCIENCES

https://doi.org/10.21608/sjsci.2023.226128.1104

Geological and Petrographical Investigation of the Neoproterozoic Basement Rocks of Wadi Arak-Wadi El Qash area, Central Eastern Desert, Egypt

Mohamed Abdelhameed[1], Abdelbaset M. Abudeif[1,*], Mohamed Abd El-Wahed[2] and Osama M.K. Kassem[3]

[1] *Geology Department, Faculty of Science, Sohag University, Sohag 82524, Egypt*
[2] *Geology Department, Faculty of Science, Tanta University, Tanta 31527, Egypt*
[3] *Geology Department, National Research Center, Al-Behoos Str., Dokki, Cairo 12622, Egypt*
[*] *Email: mohamedabdelhameed200786@gmail.com*

Received: 30th July 2023, **Revised:** 5th October 2023, **Accepted:** 7th October 2023
Published online: 24th November 2023

Abstract: The present paper focuses primarily on the geology and petrography of the Neoproterozoic basement rocks encountered in the Wadi Arak-Wadi El Qash area which is located in the extreme western side of the Central Eastern Desert of Egypt. The Wadi Arak-Wadi El Qash area is occupied and dominated by the Hammamat molasses-type sediments which overlie unconformably upon a basement of ophiolitic, arc assemblages and Dokhan volcanic, and is intruded by felsites and late to post-tectonic granites. Geological and petrographical examination revealed that the ophiolitic rocks form a NW-SE elongate belt of imbricate thrust sheets and slices of ultrabasic and basic association including serpentinites and Muweilih metabasalts together with sheared amphibolites and actinolite chlorite schist. The Arc assemblages comprise arc metavolcanic and Muweilih metaconglomerates. The island arc metavolcanic are commonly basic to intermediate with subordinate felsic composition and comprise metabasalts, metadolerite, metabasaltic andesite, metaandesite and metadacites together with their associated metaconglomerate rocks. The Muweilih metaconglomerates are intensely deformed, and their clasts were derived from pre-Dokhan volcanic rocks. The Dokhan volcanic are unmetamorphosed and embrace an association of basic to acidic lava flows together with their corresponding bedded pyroclastics. The Hammamat molasses sediments are dominated by red Igla Formation with subordinate green Shihimiya Formation. They are unmetamorphosed and classified into oligomictic and polymictic conglomerates, lithic arenites, feldspathic greywackes, siltstones, and mudstones. Felsites are characterized by plugs and dyke-like bodies and sharply intrude the Hammamat sediments. Late to post-tectonic granites are leucocratic of roughly syenogranite composition forming NW-trending pluton and intruding both Hammamat sediments and metavolcanics.
Keywords: Neoproterozoic basement rocks, Petrography, Hammamat molasses-type sediments.

1. Introduction

The Eastern Desert of Egypt represents the northwestern continuation of the Arabian-Nubian Shield (ANS). The ANS is the northern part of the East African Orogen (EAO) and forms the suture between East and West Gondwana at the northern end of the Neoproterozoic [1,2]. It is composed mainly of juvenile Neoproterozoic crust of Neoproterozoic (Cryogenian–Ediacaran, 790–560 Ma) age and was generated in association with the breakup of Rodiniaat ~800–900 Ma and closure of the Mozambique Ocean due to collision between East and West Gondwanaland at ~600 Ma. The ANS can be represented by a complex amalgam and oblique convergence of the intra-oceanic island arcs accretion, continental micro-plates, and oceanic plateaus that had resulted from theNeoproterozoic closure of the Mozambique Ocean [1-6].

The Central Eastern Desert (CED) is characterized by two distinctive tectonostratigraphic units. The lower unit comprises high-grade metamorphic gneisses, migmatites, schists, and amphibolites and is commonly referred to as the structural basement [7,8]. The upper unit includes low-grade metamorphosed ophiolite slices (serpentinites, pillow lavas, metagabbros), arc metavolcanics, arc metasediments and is commonly referred to as structural cover or the Pan-African nappes [7,9]. Both the two units were intruded by syn-tectonic calc-alkaline granites and metagabbros-diorite complex. The later stage of the crustal evolution of the CED is characterized by the eruption of the Dokhan volcanic suite which is associated with the formation of molasse-type Hammamat sedimentary rocks that were deposited in non-marine, alluvial fan/river environments [10-12]. These crustal rocks were intruded by a series of late to post-tectonic granites. The syn-tectonic granite in the CED has magmatic emplacement age of 606–614 Ma [8,13] whereas, the late to post-tectonic granites were emplaced at ca. 590–550 Ma [14,15].

The present study deals with the geological and petrographical studies of Neoproterozoic basement rocks of the Wadi Arak-Wadi El Qash area to understand the relationship between rock units during tectonic movements and minerals behavior and deformation.

2. Geologic Setting

The Wadi Arak-Wadi El Qash area lies on the extreme western side of the Central Eastern Desert of Egypt, south of

the Qift-Quseir highway asphaltic road. It is delineated by latitudes 25° 42" to 25° 56" N and longitudes 33° 32" to 33°50" E, covering an area of about 710 km^2 (Fig. 1).

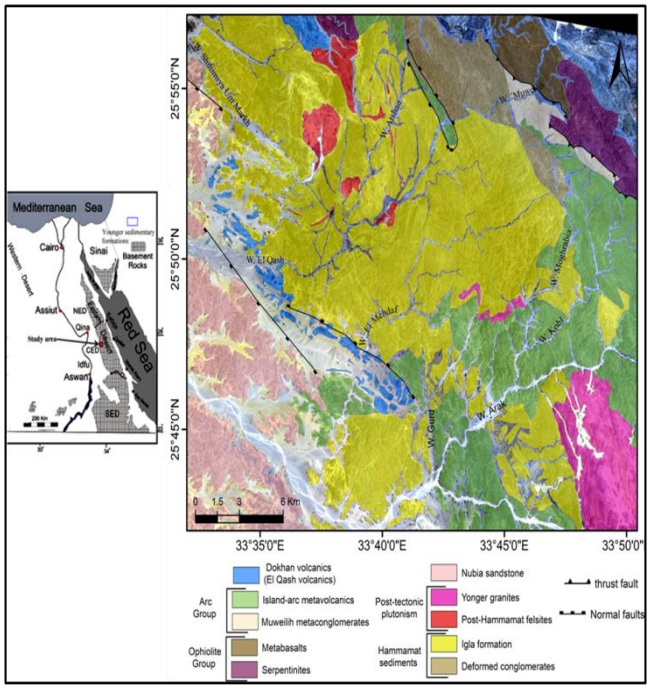

Figure 1: A geological map of the Wadi El Qash-Wadi Arak area (after 26,11). Inset map showing the location of the study area.

The study area is characterized by low to moderate topography which rises gradually in altitude eastwards. Based on field geologic mapping and field relationships, the Precambrian basement rocks of the Wadi Arak-Wadi El Qash area (Fig. 1) are chronologically arranged into ophiolite rocks (oldest), island arc metavolcanic, Muweilih metaconglomerates, Dokhan volcanics (Qash volcanics), Hammamat sediments, post-Hammamat felsites and late to post-tectonic granites (youngest).

2.1 Ophiolitic assemblages

The ophiolitic rocks form an elongated belt in an NW-SE direction with imbricate thrust sheets and slices in the northeastern corner of the study area (Figs. 1,2a). They are represented by a sequence of back-arc basin ophiolites and comprise basic and ultrabasic rocks. The ultrabasic rocks include serpentinites and related rocks. [16] suggested that the basic rocks are represented by Muweilih metabasalts including pillowed and massive non-pillowed lava flows, together with sheared amphibolites, actinolite chlorite schist, and/or chlorite epidote schist [16,17].

2.2 Island arc metavolcanics

The island arc metavolcanics are exposed commonly in the southeastern and southern parts of the study area along Wadi Arak, Wadi Kohl, and Wadi Moghrabia as well as at the entrance of Wadi El Gurd (Fig. 1). These rocks form low to moderate relief terrains with grey to greenish grey color (Fig. 2b) and comprise meta basaltic andesites, metabasalts, and metadacites together with their associated meta pyroclastics, [18]. They are unconformably overlain by the Hammamat molasse sediments. Moreover, they are intruded and thermally affected by the younger granite. A zircon fission track age of 693±40 Ma was estimated for Wadi Arak calc-alkaline metavolcanics [19].

2.3 Muweilih meta conglomerates

The Muweilih meta conglomerates, at the northeastern part of the study area (Fig. 1), represent another occurrence of the Atud conglomerate [20-22]. The Muweilih meta conglomerates and the Atud meta conglomerates were considered as sheared Hammamat conglomerates [23], however, [24] considered them as molasse-type sediments within the internal parts of the orogen. [25] divided the fragmented rocks within the Muweilih belt into three units: **(1)** The Muweilih meta conglomerates which simulate the Atud meta conglomerates, **(2)** The Um Esh olistostromal mélange and **(3)** Hammamat molasse sediments which are further subdivided into normal, tectonized and metamorphosed Hammamat. The Muweilih metaconglomerates are intensely deformed (Figs. 2c,d) and their clasts were derived from pre-Dokhan volcanic rocks, which include the metavolcanic, metagreywackes, and metamudstones with granites and marbles inclusion. The Muweilih meta conglomerates are faulted against the Hammamat conglomerates and overthrusts by Muweilih metabasalts along SW-dipping thrust. The deformed clasts of the Muweilih metaconglomerates are stretched in WNW–ESE direction and plunge 40°/S50°E (Figs. 2c,d), while the foliation strikes N50°W and dips 45°–50° SW [11,26] in the east northern part in the map.

2.4 Dokhan volcanics (Qash volcanics)

The El Qash volcanics from NW to NNW trending with low reliefed hills and are separated by wide sand wadis in the western part, especially at Wadi El Qash and Wadi El-mehdaf entrances (Fig. 1). [17] placed the Qash volcanic between the Hammamat Group and the post-Hammamat felsites while [27] considered Qash volcanics and the post-Hammamat felsites as Dokhan volcanics. [28] concluded that the Qash volcanic are lithostragraphically and petrochemically akin to the Dokhan volcanics. The El Qash volcanic comrise is an association of basic to acidic lava flows together with their corresponding bedded pyroclastics (Fig. 2e). [28] show that the lava flows of El Qash volcano comprise mainly andesites, quartz andesites, basaltic andesites, rhyodacites, and rhyolites, together with minor amounts of basalts and diabases and occasional dacites. The pyroclasts are represented by coarse agglomerate, coarse tuffs, and finely laminated tuffs of basic to acidic composition. The basalts, diabases, and andesites of El Qash volcanic evolved within the island arc or active continental setting whereas the rhyolites and rhyolites represent rift-related volcanic [28]. The Hammamate sediments rest unconformably over the pyroclasts of Qash volcanics. Interaction of the Qash volcanics and Igla sediments is not common.

2.5 Hammamate sediments

The Hammamat sediments are the most predominant rocks in the study area (Fig. 1) and are represented by three known

basins including from south to north: Arak basin, El Qash basin, and Shihimiya sub-basin.

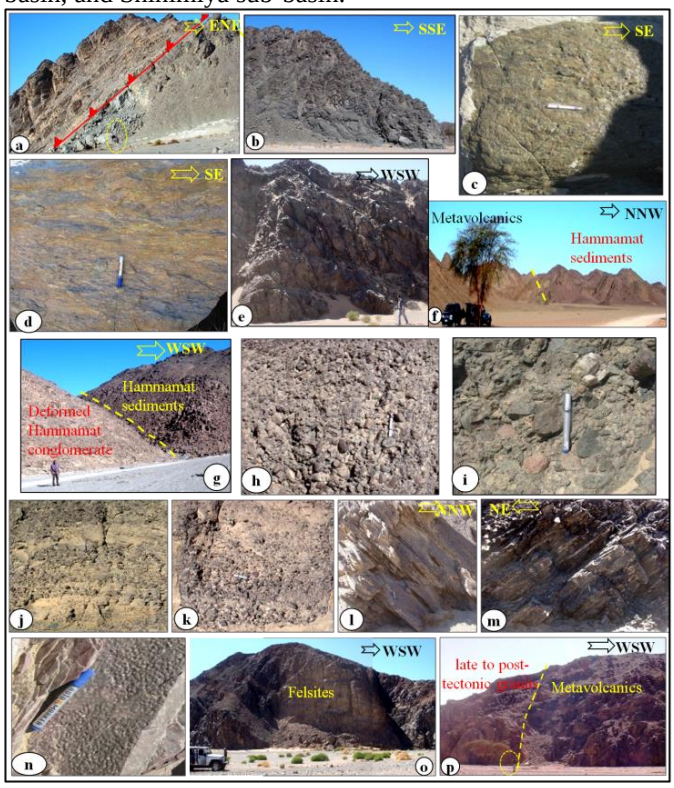

Figure 2: (a) SW-verging chlorite schists thrust over Muweilih metabasalt. **(b)** Low to moderate relieved metavolcanic rocks with grey to greenish grey color. **(c, d)** Strongly stretched and deformed pebbles oriented subparallel to the foliation planes in the Muweilih metaconglomerates. **(e)** Interbedded low to moderate relieved Dokhan volcanics with greenish grey color. **(f)** The Hammamate sediments unconformably overlie the island arc metavolcanic. **(g)** Deformed Hammamat conglomerates faulted against Hammamat sediments. **(h)** Typical red facies subrounded cobble conglomerate with clast supported. **(i)** Typical green facies subangular to subrounded boulder and cobble conglomerate with clast supported. **(j)** Repeated and recycling of interbeds conglomerates and sandstones. **(k)** Conglomerates are graded and pass upwards into pebbly sandstones. **(l,m)** well-developed fracture cleavage with attitudes of N80ºE\44º NNW and N55W\37º NE in red purple, and greenish grey sandstones respectively. **(n)** Ripple marks in red mudstone. **(o)** The Hammamate sediments are intruded by felsites plug with sharp contact. **(p)** Late to post-tectonic granite intruding the island arc metavolcanic.

The Arak basin crops out in the southern part beyond the map area lying immediately to the southern flank of the main course of Wadi Arak. The Arak basin preserves a sequence of dominantly reddish-colored clastic sediments of Igla formation. The sequence is about 2500 m, and consists of mostly pebbly (fine) conglomerate, lithic sandstone, and reddish to brick-red siltstone and mudstone. The conglomerate clasts were derived from hematite-rich Dokhan volcanic including light-coloured silicic volcanic and dark reddish brown mafic volcanic as well as reworked sedimentary clasts [29].

El Qash basin occupies the central part around Wadi El Qash and separates the Shihimiya sub-basin in the northwest from the Arak basin to the south. The basin covers the largest area compared to the other two basins. El-Qash basin is occupied mostly by the red-purple clastic sediments of the Igla Formation together with subordinate, greenish-colored clastic sediments of the Shihimiya Formation. The succession consists of basal conglomerate (720 m) followed upward by an oligomictic conglomerate (600 m), sandstone–siltstone–wacke (1,440 m), gray and red slate with siltstone intercalation (1,400 m), and finally grayish green polymictic conglomerate (1,520 m; [30]).

Shihimiya sub-basin forms a narrow NW-trending strip extending for up to 8.5 km along the main course of Wadi Shihimiya Um Markha in the northwestern part of the map area and represents the south-westernmost extension of Wadi Hammamat molasse clastic sediments. Unlike El Qash and Arak molasse clastic sedimentary basins, the Shihimiya sub-basin is dominated by greenish-colored clastic sediments of the Shihimiya formation, with a minor amount of Igla formation, which consists of siltstone, lithic sandstones-wackes and a unit of polygenetic conglomerates [16].

Generally, the conglomerate varies in color according to composition from reddish gray to grayish green, poorly to moderately sorted and commonly undeformed. It consists of rounded to sub-rounded and subangular boulders, cobbles, and pebble clasts. In reddish conglomerates varieties, the gravel clasts include light-colored silicic volcanic and dark reddish brown mafic volcanic and sedimentary clasts, whereas in green conglomerates the gravels are mostly volcanic and metavolcanic with subordinate granite clasts. Some conglomerates are poor in matrix and clast-supported (Figs. 2 h, i) while others are matrix-supported. Conglomerates are interbedded (Fig. 2j) or graded and pass upwards into pebbly sandstones (Fig. 2k). The sandstones and siltstones show similar characteristics with different grain sizes. They were characterized by well-developed fracture cleavage with N80°E\44°NNW and N55°W\37°NE directions. Generally, they are red-purple, brick red to greyish green in colorand unmetamorphosed. Sometimes, they are pebbly and exhibit primary sedimentary structures such as bedding, lamination, graded bedding, ripple marks and rain prints that are well developed and preserved (Figs. 2 m,n).

The molasses sediments rest unconformably over the island arc metavolcanic (Fig. 2f) and the Dokhan volcanic while they are faulted against the deformed Hammamate conglomerates (Fig. 2g) and intruded by post-Hammamat felsites (Fig. 2o) as well as by late to post-tectonic granitoid. The deformed Hammamat conglomerates, which lie in the northeastern part of the map area, are poorly sorted and their clasts were derived mainly from within-plate island arc or active continental margin volcanic rocks and alkaline post-orogenic leucocratic granites [25]. The deformed Hammamat conglomerates faulted the Muweilihmetaconglomerates.

2.6 Post-Hammamat felsites

The post-Hammamat felsites occur as small masses, plugs, and dyke-like bodies and intrude the Igla sediments with sharp contact (Fig. 2o), particularly around Wadi El Qash and Wadi Atshan.

2.7 Late to post-tectonic granites

[14] Suggested that the late to post-tectonic granites form a NW-SE trending pluton in the southeastern part, but extend further southerly for several kilometers outside the study area. They are intruding on the island arc metavolcanic (Fig. 2p) as well as Igla sediments with sharp contact. Rb/Sr age range of 610-550 Ma for the late to post-tectonic granites [31].

3. Materials and methods:

Ninety representative samples of the various rock units have been collected with their location determined by Geographic Positioning System (GPS) for petrographical and mineralogical studies. The collected samples were cut and prepared into thin sections and examined microscopically by using a transmitted polarized microscope to throw light on their mineral composition and petrographic features.

The field mapping and petrographic studies of the rock samples were done in order to delineate the different rock types present in the area and to update or improve upon the previous works on the geology of the area.

4. Results and Discussion:

4.1 Ophiolitic assemblages

Ophiolitic rocks in the study area are petrographically distinguished into:

Serpentinite rocks: serpentinite rocks are greenish black to dark brownish green color, medium to fine-grained and massive. Microscopically, they are composed mainly of chrysotile, lizardite, and talc with variable amounts of chromite and magnetite as accessory minerals. Mesh texture is the unique texture characterized by these rocks (Fig. 3a). Chrysotile occurs as a cross fiber veinlets traversing the matrix, and some crystals of chrysotile partially and completely altered to talc mineral forms microcrystalline aggregates display high interference color. Lizardite occurs as fine-grained elongated microcrystals forming a bundle-like form. Talc found in the groundmass forming fine to medium-grained plates of high interference color replacing serpentine minerals. Chromite is a subordinate constituent and occurs as anhedral crystals, sub-rounded and irregular grains of dark red to deep reddish-brown color, cracked and it is slightly replaced by magnetite along the margins in some slices where magnetite is darker than chromite. Magnetite is represented by fine-grained discrete aggregates and sparse patches distributed throughout the rock.

Metabasalts (Fig. 4) are greenish-grey in color, fine-grained and massive. Microscopically, they are composed of a subequal portion of plagioclase, actinolitic hornblende, and actinolite together with chlorite, epidote, zoisite, and iron oxides. Ophitoblast, subophitoblast, and intergranular textures are preserved (Fig. 3b). Plagioclase (An38-45) occurs as subhedral to euhedral thin lath, up to 0.8 mm long and forms about 45-60 vol% of the rock, showing albite and albite-carlsbad twins and partiallysaussuritized into aggregates of epidote andziosite. Generally, plagioclase laths are arranged in triangular patterns defining the intergranular texture. Actinolitic hornblende occurs as subhedral prismatic crystals, up to 1.2 mm long, with fibrous terminations. It is pseudomorphs after pyroxene, green in color, and moderately pleochroic from yellowish green to green. Actinolite forms subhedral to anhedral slender crystals, up to 0.6 mm long, and fibers aggregates of pale green color and faintly pleochroic. Both actinolitic hornblende and actinolite are partly altered to chlorite and iron oxides. Chlorite occurs as small flakes associated with and replacing actinolite. It is pale green in color and faintly pleochroic. Epidote and ziosite from anhedral granular aggregates associated with and replacing plagioclase and less commonly actinolite. Iron oxides occur as minute crystals disseminated throughout the rock and are also associated with and enclosed within the mafic minerals.

Sheared amphibolite rocks are medium-grained, greenish-grey in color, and foliated. They are composed mainly of plagioclase, actinolitic hornblende, and actinolite together with chlorite, calcite, minor epidote, and iron oxides. Generally, the foliation is marked by strong alignment of the mafic constituents (Fig. 3c). Plagioclase occurs as subhedral to prismatic crystals, up to 0.5x1.2 mm, showing albite and albite-carlsbad twins and moderately saussuritized to epidote, sericite, and calcite. They are mostly affected by deformation such as microfractures and bending of lamellar twinning, and others are fragmented. Actinolitic hornblende and actinolite occur as subhedral prismatic crystals, up to 0.4x1.6 mm with fibers terminations and fibers aggregates aligned in subparallel orientation defining the main foliation. It is pale green in color, faintly pleochroic, and frequently altered to chlorite. Chlorite occurs as subhedral to anhedral flakes associating and replacing actinolite. It is pale green in color and faintly pleochroic. Calcite forms are lensodial and stretched crystals, up to 2 mm long, with their long axes arranged subparallel to the general foliation. Iron oxides commonly form stretched and elongated grains, up to 0.6 mm long, disposed in subparallelism.

Actinolite chlorite schists are strongly foliated rocks of greyish-green color. They are composed of plagioclase, actinolite, chlorite, epidote, calcite, and iron oxides. The schistosity is marked by the subparallel alignment of the mafic constituents (Fig. 3d). Plagioclase forms subhedral saussuritized thin laths disseminated at random. Actinolite forms subhedral prisms, up to 0.6 mm long, and fibers aggregates allied with their longer axes in subparallel orientation. They are wrapped around plagioclase and frequently altered to chlorite, epidote, and calcite. Chlorite occurs as patches and small flakes commonly associated with actinolite. Epidote forms subhedral to anhedral crystals commonly associated with actinolite and chlorite. Iron oxides forms irregular crystals disseminated throughout the rock and also enclosed within the mafic minerals.

4.2 Island arcassembelages

The petrographical descriptions of these metavolcanic include the following varieties: metabasalts, meta dolerite, meta basaltic andesite, meta-andesite, and their equivalent metapyroclastics.

Metabasalts (Fig. 4) are greyish-green in color, fine-grained and massive. They consist of plagioclase, chlorite, and calcite patches pseudomorphs after pyroxene, with dispersed iron oxides. Sericite, kaolinite, and minor epidote present alteration

products of plagioclase laths. Ophitoblast, subophitoblast, and intergranular textures are still preserved (Figs. 3 e,f). Plagioclase (An40- 48) (44–50 vol.%) occurs as subhedral to euhedral small laths, up to 0.6 mm long, showing albite and albite-carlsbad twins and frequently saussuritized. Some plagioclase laths enclosed within chlorite and calcite depict the inherited ophitoblast, and subophitoblast textures. Chlorite occurs as subhedral to anhedral flakes and patches up to 0.3x0.7 mm, pseudomorphs after pyroxene. It is pale greenish in color, faintly pleochroic, and displays anomalous blue interference color. Calcite forms subhedral to anhedral irregular patches with a creamy color and sometimes enclosed plagioclase laths. Iron oxides form fine granules dispersed throughout the rock or associated and enclosed within chlorite.

Metadolerite is medium-grained and massive with a grayish-green color. They are composed essentially of plagioclase, actinolitic hornblende, and actinolite with minor quartz. Chlorite, calcite, epidote, and sericite are the main secondary minerals, whereas iron oxides are accessories. Intergranular, ophitoblast, and subophitoblast textures are common (Fig. 3g). Plagioclase (An20-35) forms euhedral to subhedral prismatic crystals, up to 0.3x1.4 mm, arranged in triangular habit manifesting the intergranular texture. They are twinned according to albite and combined albite-carlsbad laws; some are zoned, and variably altered to epidote and calcite. Hornblende forms subhedral prismatic crystals, up to 0.4x1.2 mm, of green color and strongly pleochroic from yellowish green to dark green. Some hornblende crystals are altered to actinolite and chlorite. Actinolitic hornblende and actinolite occur as subhedral prismatic crystals, up to 0.5x 1.6 mm, and fibers aggregates. It is pale green in color, faintly pleochroic and frequently altered to chlorite and calcite (Fig. 3h). Chlorite occurs as subhedral to anhedral flakes and irregural patches, developed at the expense of amphiboles, with blue interference color. Calcite forms are suhedral to anhedral sporadic grains that altered from hornblende and actinolite crystals due to the uralitization process. Iron oxides occur as subhedral to anhedral irregular and elongated grains, up to 0.4 mm long, commonly restricted and enclosed within mafic constitutes.

Metabasaltic-andesites are transitional between metabasalt and metaandesites. They consist mainly of microphenocrysts of plagioclase and chlorite, pseudomorphs after pyroxene, set in a fluidal groundmass of microlithic plagioclase together with chlorite, epidote and iron oxides (Fig. 3i). Plagioclase is distinguished into two generations. The earlier one forms idiomorphic to xenomorphic phenocrysts, up to 0.4x0.8 mm intensely saussuritized and kaolinitized, and consequently their twinning is masked, and some crystals are zoned with altered core and fresh rime. The second one is represented by flow-oriented small plagioclase laths and microlites, up to 0.3 mm long, in groundmass forming a fluidal pattern. Chlorite occurs as subhedral prismatic crystals to anhedral patches, up to 0.6x1 mm, and pseudomorphs after pyroxene. It is a pale greenish color with an anomalous blue interference color. Epidote forms granular aggregates replacing plagioclase crystals and concentrating in the groundmass. Iron oxides occur as fine granules dispersed in the groundmass.

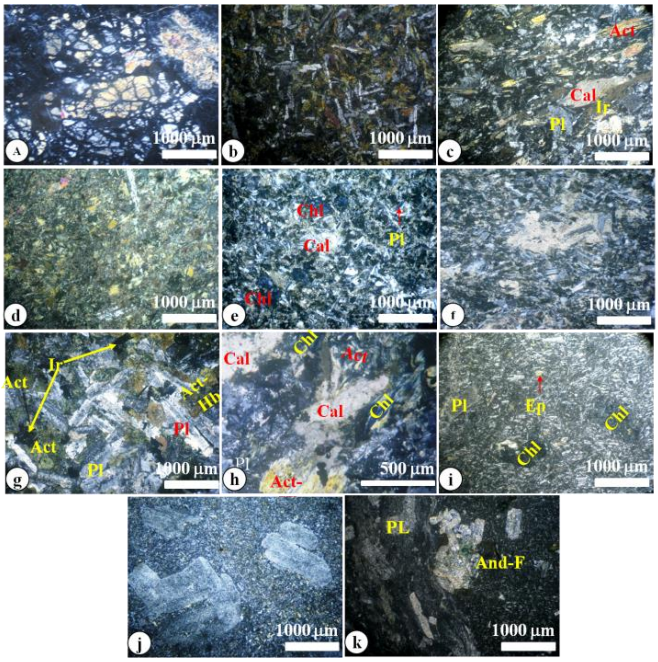

Figure 3: **(a)** Mesh texture show relicts of olivine crystal in serpentinite. **(b)** Intergranular texure in metabasalt. **(c)** Foliation in amphibolite is defined by subparallel alignment of actinolite, chlorite, fragmented plagioclase and stretched calcite and opaque minerals. **(d)** Aligned abundant slender actinolite crystals defining a foliation in actinolite chloriteschist. **(e)** Altered plagioclase laths, calcite andchlorite patches pseudomorphs after pyroxene in metabasalt. **(f)** Ophitoblast and subophitoblast texture in metabasalr. **(g)** Metadolorite, with diabasic texture, consisting mainly of plagioclase, hornblende and actinolite together with iron oxides. **(h)** Calcite and chlorite plates associated with altered actinolite in metabolite. **(i)** Metabasaltic andesite with flow-oriented plagioclase laths and chlorite pseudomorphs of pyroxene phenocrysts. **(j)** Metaandesite with altered plagioclase phenocrysts embedded in a fine-grained groundmass identifying the porphyritic texture. **(k)** Lithic metaandesite and altered plagioclase fragments set in tuffaceoustuffaceous matrix in lapillimetatuffs.

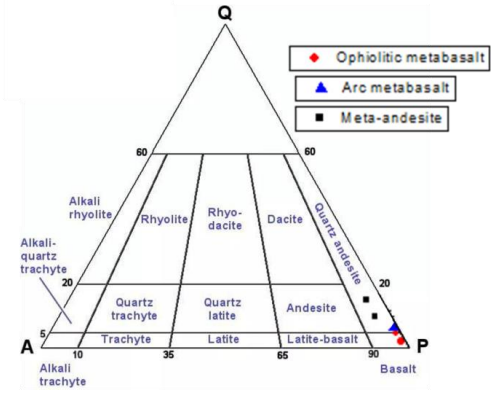

Figure 4: QAP modal classification diagram after [32] for some volcanic rocks.

Meta-andesites (Fig. 4) are commonly metaporphyritic with greenish-grey color. They are composed of altered plagioclase phenocrysts embedded in fine-grained groundmass made up of fine plagioclase laths, actinolite fibers, minor quartz, epidote and iron oxides (Fig. 3j). Plagioclase (42–47 vol.%) forms subhedral phenocrysts, up to 0.8x1.6 mm, with turbid and

cloudy appearance due to intense alteration to epidote and kaolinite. However, the less altered plagioclase crystals display polysynthetic twins. It also occurs as small laths and microliths in the groundmass. Actinolite is commonly concentrated in the groundmass as acicular needle-like and fiber aggregates. Quartz (10–16 vol.%) forms intergranular fine grains and aggregates with water-clear surface in the groundmass. Iron oxides occur as anhedral granules disseminated in the groundmass.

Intermediate lithic crystal lapilli metatuffs are medium to fine-grained, greenish-grey in color, and massive. They consist of lithic fragments and crystal fragments commonly of plagioclase and rare of quartz set in fine-grained tuffaceous matrix (Fig. **3k**). Lithic fragments form subangular to subrounded fragments, up to 3×3.5 mm, represented by porphyritic metaandesites that composed mainly of altered plagioclase phenocrysts embedded in fine-grained groundmass of small plagioclase laths and opaques. Plagioclase forms subhedral to anhedral clastic gains, up to 0.4×1.2 mm, displaying albite twinning; however, some crystals are masked due to the saussuritization process. The fine-grained tuffaceous matrix is composed of plagioclase, sericite, calcite, epidote, iron oxides, and dust material.

Intermediate crystal metatuff is fine-grained, grey to greenish grey color, and massive to laminated. They consist of plagioclase crystal fragments embedded in a fine-grained tuffaceous matrix formed of plagioclase, epidote, iron oxides, minor quartz, and dust materials (Fig. **5a**). Plagioclase forms subhedral to anhedral crystal fragments, up to 0.7×0.36 mm, and are moderately to strongly altered to epidote and calcite. Quartz is less common and forms subhedral small grains of water with clear surfaces in the tuffaceous matrix. Epidote forms anhedral aggregates of pale olive color and high birefringence disseminated in the tuffaceous matrix.

4.3 Muweilih meta conglomerates

These rocks are greenish-grey in color, coarse-grained and moderately to strongly foliated. They consist mainly of lithic fragments and crystal fragments commonly of quartz and plagioclase set in a moderately to strongly schistose fine-grained matrix composed of quartz, plagioclase, sericite, calcite, chlorite, epidote, and iron oxides. Lithic fragments, up to 3.2×3 mm, comprise commonly metavolcanic (including metabasalt, basaltic metaandesite, porphyritic meta-andesite, and metadacite) and reworked metasediments. The lithic fragments are stretched and elongated parallel to the foliation planes. Quartz usually forms stretched lensoidal (augen-shaped) crystals exhibiting strongly undulate extinction and sometimes partially to completely dynamically recrystallized into subgrains. Plagioclase forms angular to subround crystals, mostly altered and clouded with sericite and clay materials and usually fractured and cracked (Figs. **5 b,c**).

Metagreywakes are greenish-grey in color, fine to medium-grained and moderately to strongly foliated. They consist of subangular to subrounded detrital grains commonly of quartz and plagioclase embedded and stretched in a schistose matrix of fine-grained quartz, plagioclase, sericite, chlorite, epidote, calcite, and iron oxides.

4.4 Dokhan Volcanics (El Qash volcanic)

These rocks are distinguished commonly into:

Intermediate lithic crystal lapilli tuffs are medium to fine-grained, greenish-grey in color, and massive. They consist of lithic fragments and crystal fragments commonly of plagioclase and rare of quartz set in a fine-grained tuffaceous matrix. Lithic fragments form subangular to subrounded plagioclase and rare quartz set in a fine-grained tuffaceous matrix. Lithic fragments form subangular to subrounded fragments, up to 3×3.5 mm, represented mainly by basaltic andesite and porphyritic andesite. Plagioclase forms subhedral to anhedral clastic gains, up to 0.4×1.2 mm, displaying albite twinning and sometimes partially altered to saussurite. The fine-grained tuffaceous matrix is composed of plagioclase, calcite patches, minor epidote, iron oxides, and dust materials (Fig. **5d**).

Acidic lithic crystal lapilli tuffs are medium to fine-grained, greenish-grey in color, and massive. They consist of angular to subrounded crystal fragments of quartz and plagioclase and lithic fragments set in fine-grained tuffaceous matrix of quartz and plagioclase together with sericite, calcite, epidote, iron oxides and dust material (Fig. **5e**). The lithic fragments are represented by porphyritic dacite that composed mainly of quartz and plagioclase phenocrysts embedded in cryptocrystalline groundmass. Quartz occurs as angular to subrounded clastic crystals displaying water-clear surface. Plagioclase forms subhedral to anhedral clastic gains, up to 0.4×1.2 mm, displaying albite twinning; however, some crystals are masked due to the saussuritization process.

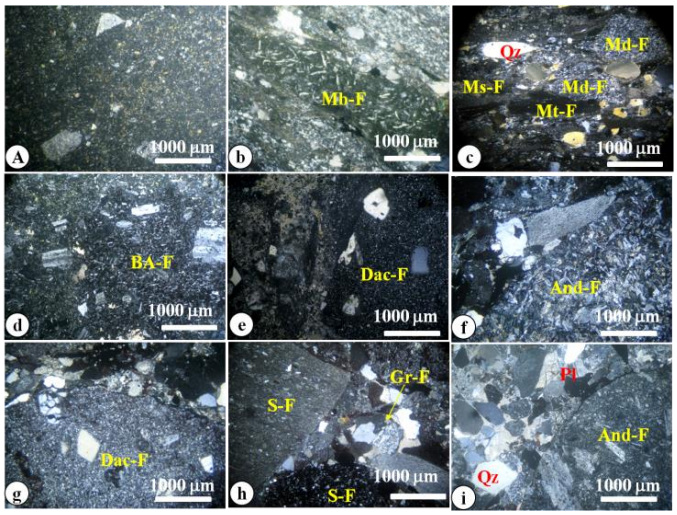

Figure 5: (a) Altered plagioclase crystal fragments set in tuffaceous matrix in crystal metatuffs. **(b,c)** stretched lithic fragments of metabasalt in **(b)**, metadacite, metatuff, and metasediments together with stretched quartz crystals set in schistose fine-grained matrix in Muweilihmetaconglomerates. **(d)** Lithic andesite and plagioclase fragments set tuffaceous matrix in intermediate lithic crystal lapilli tuffs. **(e)** Dacite lithic fragment set tuffaceous matrix in acidic lapilli tuffs. **(f,h)** Lithic fragments of andesite in **(f)**, dacite in **(g),** and granophyres and reworked hematitic siltstone in **(h)** in the conglomerate. **(i)** Lithic andesite clast and plagioclase and quartz crystal fragments in lithic arenites.

4.5 Hammamat sediments

Petrographically, the Hammamat sediments are distinguished into a conglomerate, lithic arenite, feldspathic greywacke, siltstone, and mudstone.

Conglomerates are massive with greenish grey to reddish-purple color. They consist of subangular, subrounded to rounded boulders, cobbles, and pebbles lithic fragments set in a sandy-sized matrix composed mainly of quartz and plagioclase together with calcite, minor epidote, and iron oxides. In reddish conglomerates varieties, the lithic fragments are mostly pebbles to cobbles in size and represented mainly by Dokhan-type volcanic (commonly of andesites and dacites) and reworked sedimentary rocks including siltstones, mudstones, and sandstones, in addition to rare or less abundant microgravity (granophyres) fragments (Figs. **5 f,g,h**). The green conglomerate clasts are diverse and include arc metavolcanic (metabasalt, metaandesite, metadacite, and metatuffs) and Dokhan volcanic in addition to younger granites, older granite, epidote and quartz.

Lithic arenites are red-purple in color, medium-grained, and composed mainly of clastic grains of quartz, plagioclase and minor alkali feldspars together with a subordinate amount of lithic fragments embedded in a fine-grained matrix of plagioclase, quartz, calcite, sericite, minor chlorite, and iron oxides (Figs. **5 I,a**). Quartz occurs as subrounded clastic crystals with clear surfaces, locally dissected by fractures filled with calcite, and shows weakly undulose extinction. Plagioclase forms subhedral clastic grains with albite twinning and is frequently saussuritized and serialized. Alkali feldspars are less common and represented by microperthite and microcline. They are slightly turbid with sericite and clay. The lithic fragments (up to 2.00 mm in length) include mainly volcanic (e.g., porphyritic andesite) and reworked sedimentary (mainly of hematitic siltstone) clasts.

Feldspathic greywackes show chlorite, epidote, subordinate mica, and minor lithic fragments embedded in a much finer silty-sized matrix of quartz and plagioclase together with calcite, chlorite, sericite, epidote, iron oxides and clay minerals (Fig. **6b**). In some varieties, the clastic grains of greywackes are cemented by matrix rich in calcite and carbonate materials. Quartz forms subrounded clear-surfaced grains, sometimes exhibiting wavy extinction and corroded by the matrix. Plagioclase forms subangular saussuritized clasts with albite twining and locally microfracture with bending of lamellar twinning (Fig. **6c**). Mica is less abundant and represented commonly by muscovite and minor biotite. Biotite forms subhedral detrital flakes, up to 1.2 mm long, strongly pleochroic from dark brown to pale brownish yellow color, and frequently chloritized. Muscovite occurs as subhedral flakes, interspersed between quartz and plagioclase, sometimes bent and displays wavy extinction (Fig. **6d**). Chlorite occurs as anhedral to subhedral flakes of pale green color and faintly pleochroic (Fig. **6e**). Calcite forms anhedral patches replacing plagioclase crystals and concentrated in the matrix. Epidote occurs as anhedral granules commonly associated with altered plagioclase and concentrated in the matrix (Fig. **6e**).

Siltstones are fine-grained, massive to laminated, and display brick red to reddish brown and greenish grey colors. They consist of angular to subrounded silt-size particles of quart brick red to reddish brown and greenish grey colors. They consist of angular to subrounded silt-size particles of quartz and subordinate plagioclase together with sericite, minor epidote, and iron oxides set in a finer clayey matrix. In laminated varieties, the siltstone displays marked quartz and subordinate plagioclase together with sericite, minor epidote, and iron oxides set in a finer clayey matrix. In laminated varieties, the siltstone display marked lamination with alternating silty and fine-grained sandy laminae (Fig. **6f**).

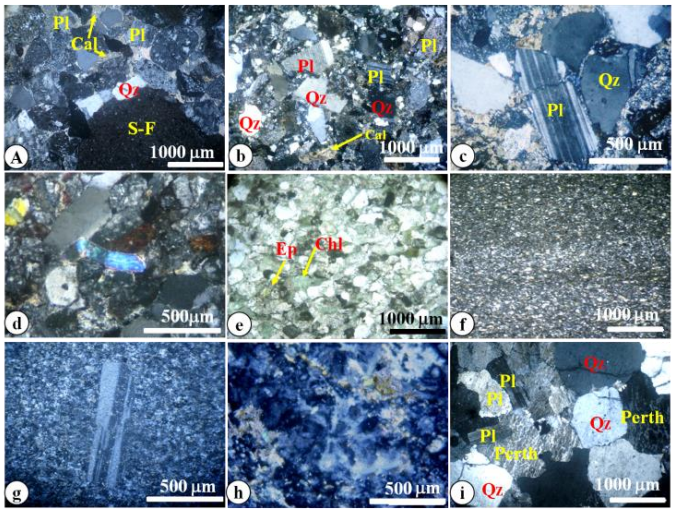

Figure 6: (a) Reworked hematitic siltstone lithic fragment set in a sand-size matrix of plagioclase and quartz together within interstitial calcite crystal fragments in lithic arenites. **(b)** Red purple feldspathic greywackes with quartz and plagioclase clastic grains embedded in a fine-grained matrix rich in iron oxides. **(c)** Microfaulting and cracks within plagioclase and quartz in feldspathic greywackes. **(d)** Bent muscovite in feldspathic greywackes. **(e)** Epidote and detrital chlorite in green feldspathic greywackes. **(f)** Intercalating silt-sized quartz and plagioclase-rich light and iron oxides and sericite-rich dark laminae in red siltstone. **(g)** Long prismatic plagioclase phenocryst embedded in a fine-grained groundmass of quartz and alkali feldspars in felsite. **(h)** Spherulitic texture in felsite. **(i)** Hypidiomorphic texture in syenogranite composedcomposed of quartz, perthite, and plagioclase crystals.

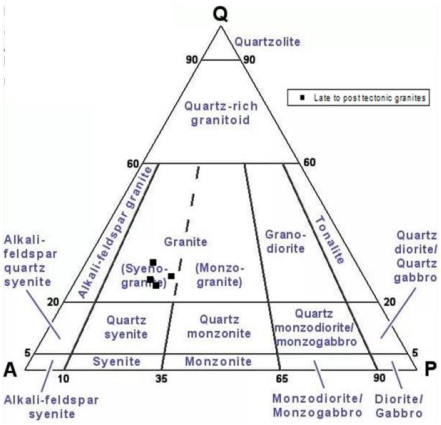

Figure 7: QAP modal classification diagram after [32] for late to post-tectonic granites.

4.6 Post-Hammamat felsites

They are characterized by buff to pinkish grey color, fine-grained and massive. They are composed of plagioclase phenocrysts embedded in fine-grained groundmass composed of quartz and alkali feldspars with subordinate iron oxides. These rocks typically display porphyritic, glomeroporphyritic, and spherulitic textures (Figs. **6 g,h**).

4.7 Late to post-tectonic granites

They are represented commonly by leucocratic perthitic syenogranite (Fig. **7**) which is pinkish-grey in color, coarse-grained, and massive [**11**]. They are composed essentially of quartz, feldspars (both microcline and orthoclase), and subordinate plagioclase together with a lesser amount of biotite. Sericite, kaolinite, minor calcite, and chlorite are secondary minerals whereas iron oxides represent the main accessory minerals. Hypidomorphic and perthitic textures are characteristic (Fig. **6i**). Quartz (23-31 vol%) occurs as subhedral to anhedral crystals, up to 2 to 3 mm across, filling the interstitial space between the perthites and plagioclase and showing corrosive action against them. It is locally fractured and exhibits weakly undulose extinction. Feldspars (44–50 vol.%) are represented by orthoclase and microcline crystals with strings, veins, and patches types of perthite. Orthoclase occurs as subhedral tabular crystals, up to 2.2 × 3.4 mm, and simply twinned. Microcline occurs as subhedral tabular crystals, up to 2.7 × 3.2 mm, with the characteristic cross-hatching twining and enclosing poikilitically small plagioclase laths. Both orthoclase and microcline crystals are partially altered to sericite, and kaolinite and stained by hematite. Plagioclase (An13–25) forms (15-22 vol.%) subhedral tabular crystals, up to 0.8 x 1.6 mm, twinned according to the albite law and slightly kaolinized and sericitized. Sometimes, it is brittly deformed and dissected by microfractures. Biotite is less common and forms subhedral flakes, up to 0.8 mm long, strongly pleochroic from dark brown to pale brownish yellow color, and frequently altered to chlorite along cleavage planes and margins. Sericite and calcite present as minute microcrystalline aggregates as alteration products of plagioclase and feldspar crystals.

5. Conclusion

The Wadi Arak-Wadi El Qash area is predominantly built up of Hammamat clastic sedimentary rocks which rest unconformably over island-arc assemblages and Dokhan volcanic and intruding by felsites and late to post-tectonic granites. Field relations and observations supplemented by petrographical studies revealed that the ophiolitic rocks form a NW-SE elongate belt of imbricate thrust sheets and slices of ultrabasic and basic association including serpentinites and Muweilih metabasalts together with sheared amphibolites and actinolite chlorite schist. The island arc metavolcanic range in composition from basic-intermediate to acidic and comprises metabasalts, meta dolerite, metabasaltic andesite, meta andesite, and metadacites together with their associated meta pyroclastics. The Muweilih meta conglomerates are intensely deformed and their clasts were derived from pre-Dokhan volcanic rocks. The Dokhan volcanic comprises an association of basic to acidic lava flows together with their corresponding bedded pyroclastics. The Hammamat molasses sediments are dominated by the red Igla Formation with subordinate green Shihimiya Formation and are classified into oligomictic and polymictic conglomerates, lithic arenites, feldspathic greywackes, siltstones, and mudstones.

CRediT authorship contribution statement:

"Conceptualization, Mohamed Abd El-Wahed and Osama M.K. Kassem methodology, Mohamed Abdelhameed, and Abdelbaset Abudeif; software, Mohamed Abd El-Wahed, and Osama M.K. Kassem; validation, Abdelbaset Abudeif, Mohamed Abd El-Wahed, and Osama M.K. Kassem; formal analysis and investigation; Mohamed Abdelhameed, Mohamed Abd El-Wahed, and Osama M.K. Kassem; resources, Abdelbaset Abudeif.; data curation, Osama M.K Kassem; writing—original draft preparation, Mohamed Abdelhameed.; writing—review and editing, Mohamed Abd El-Wahed, Abdelbaset Abudeif, and Osama M.K. Kassem; visualization, Abdelbaset Abudeif; supervision, Abdelbaset Abudeif, Mohamed Abd El-Wahed, and Osama M.K. Kassem. All authors have read and agreed to the published version of the manuscript."

Data availability statement

The data used to support the findings of this study are available from the corresponding author upon request.

Declaration of competing interest

The authors declare that they have no known competing financial interests or personal relationships that could have appeared to influence the work reported in this paper.

References

[1] Stern, R.J., *Annual Review of Earth and Planetary Sciences*, 22 (1994) 319–351.
[2] Stern, R.J., *J. Afr. Earth Sci*, 34 (2002) 109–117.
[3] Johnson, P.R., Woldehaimanot, B., *Geol., Soc., London, Spec., Publ.*, 206 (2003) 289–325.
[4] Meert, J.G., *Tectonophysics*, 362 (2003) 1–40.
[5] Johnson, P.R., Andresen, A., Collins, A.S., Fowler, A.R., Fritz, H., Ghebreab, W., Kusky, T., Stern, R.J., *J., Afr., Earth Sci.*, 61 (2011) 167–232.
[6] Fritz, H., Abdelsalam, M., Ali, K.A., Bingen, B., Collins, A.S., Fowler, A.R., Ghebreab, W., Hauzenberger, C.A., Johnson, P.R., Kusky, T.M., Macey, P., Muhongo, S., Stern, R.G., Viola, G., *J., Afr., Earth Sci.*, 86 (2013) 65–106.
[8] Loizenbauer, J., Wallbrecher, E., Fntz, H., Neumayr, P., Khudeir, A.A., Kloetzil, U, *Precambr. Res.*, 110 (2001) 357–383.
[9] Fritz, H., Wallbrecher, E., Khudier, A.A., Abu El Ela, F., Dallmeyer, R.D., *J., Afr., Earth Sci.*, 23 (1996) 311–329.
[10] Grothaus, B.D., Eppler, D., Ehrlich, R., *Ann., Geol., Surv.*, 9 (1979) 231–245.
[11] Abd El-Wahed, M.A., *J., Geosci.*, 3 (2010) 1–26.
[12] Bezenjania, R.N., Pease, V., Whitehouse, M.J., Shalaby, M.H., Kadi, K.A., Kozdroj, W., *Precambr. Res.*, 245 (2014) 225–243.
[13] Andresen, A., Augland, L.E., Boghdady, G.Y., Lundmark, A.M., Elnady, O.M., Hassan, M.A., Abu El-Rus, M.A., *J., Afr., Earth Sci.*, 57 (2010) 413–422.
[16] Akaad, M.K., Noweir, A.M., *Institute of Applied Geology, Jeddah, Saudi Arabia*, 3 (1980) 127–135.

[17] Akaad, M.K., Abu El Ela, A.m., *Egyptian journal of Geology*, 40 (1996) 321–349.
[18] Makroum, F.M., Assaf, H.S., Saleh, G.M., *Egyptian Journal of Geology*, 45 (2001) 51–64.
[20] Akaad, M.K., Noweir, A.M., *Bulletin of Faculty of Science, AssiutUniversity, Egypt*, 7 (1964) 31–48.
[21] Akaad, M.K., Abu El Ela, A.m., *Ain-Shams University, Egypt, Earth Science*, 4 (1990) 1–21.
[22] Akaad, M.K., *Geological Survey of Egypt Paper*, 71 (1996).
[23] Ries, A.C., Shackleton, R.M., Graham, R.H., Fitches, W.R., *J. Geol., Soc., London*, 140 (1983) 75–95.
[25] Abu El-Ela, A.M., El-Bahariya, G.A., *Egypt J., Geol.*, 41(2A) (1997) 5–35.
[26] Abd El-Wahed MA, *Annals of the Egyptian Geological Survey*, 27 (2004) 79–108.
[28] Abu El-Ela, A.M., *Delta Journal Of Science*, 20 (1996) 145–171.
[29] Fowler, A., Osman, A.F., *Gondwana Res.*, 23 (2013) 1511–1534.
[31] Moghazi, A.M., *Geological Magazine*, 136 (1999) 285–300.
[32] Streckeisen, A.L., *A provisional attempt: Neues Jahrbuch fur Mineralogie, Monatshefte*, 1 (1976) 1–15.

For book:

[7] El-Gaby, S., List, F.K., Tehrani, R., The basement complex of the Eastern Desert and Sinai. In: Said, R. (Ed.), The Geology of Egypt. A.A. Balkema, Rotterdam, 1990.
[14] Hassan, M.A., Hashad, A.H., Precambrian of Egypt. In: Said, R. (Ed.), TheGeology of Egypt. Balkema, Rotterdam, 1990.
[15] Rice, A.H.N., Osman, A.F., Abdeen, M.M., Sadek, M.F., Ragab, A.I., Preliminary comparison of six late-to post-Pan-African molasse basins, E. Desert, Egypt. In Thorweihe, U., Schandelmeier, H. (Eds.), Geoscientific Research in Northeast Africa. Proceedings of the International Conference on Geoscientific Research in North Africa. Balkema, Rotterdam, 1993.
[19] Dixon, T.H., The evolution of the continental crust in the Late Precambrian Egyptian Shield.Ph.D. thesis, University of California, San Diego, 1979.
[24] Wallbrecher, E., Fritz, H., Khudeir, A.A.,Farahat, F., Kinematics of Pan-African thrusting and extension in Egypt. In: Thorweihe U, Schandehneier H (eds) Geoscientific Research in Northeast Africa. Balkema, Rotterdam, pp 1993.
[27] El-Gaby, S., List, F.K., Tehrani, R., Geology, evolution and metallogenesis of the Pan-African Belt in Egypt. In: El-Gaby, S., Greiling, R.O. (Eds.), The Pan-African Belt of Northeast Africa and Adjacent Areas. Vieweg&Sohn,Weisbaden, 1988.
[30] Assaf, H.S., Structure and radioactive mineralization of Wadi Arak area, Eastern Desert, Egypt.Ph.D. dissertation, Ain Shams University, Cairo, Egypt, 1973.